Electronic Supplementary Material (ESI) for Environmental Science: Processes & Impacts.

Supplementary Information

Extending Surface Enhanced Raman Spectroscopy (SERS) of Atmospheric Aerosol Particles to the Accumulation Mode (150-800 nm)

Peter N. Tirella[1], Rebecca L. Craig[1], Darrell B. Tubbs[1], Nicole E. Olson[1], Ziying Lei[2], Andrew P. Ault[1,2*]

[1]Department of Chemistry, University of Michigan, Ann Arbor, Michigan, 48109
[2]Department of Environmental Health Sciences, University of Michigan, Ann Arbor, Michigan, 48109

*corresponding author's e-mail: aulta@umich.edu

Testing Ag SERS Substrates

Several different Ag SERS substrates were tested for their application to aerosol particle studies. Ag nanoparticles (AgNPs) were synthesized according to the method by Leopold and Lendl.[1] Briefly, a mixture of NaOH and hydroxylamine hydrochloride was added to a solution of $AgNO_3$. The size of the resulting nanoparticles depended on the speed of mixing of the two solutions. Rapid mixing led to smaller nanoparticles (~30 nm) while mixing dropwise led to larger nanoparticles (~60 nm). Ag bipyramidal nanoparticles were synthesized according to the method by Zhang et al.[2] Briefly, a mixture of $AgNO_3$, sodium citrate, BSPP, and NaOH was irradiated with a mercury lamp for 18 hours. The resulting colloidal solutions of AgNPs and Ag bipyramids were drop-coated onto clean quartz slides and dried in a desiccator to create SERS substrates in the same manner as Craig et al.[3]

A NanoSight/Malvern nanoparticle tracking analysis (NTA) system was used to measure the size (hydrodynamic diameter) of the nanoparticles in solution based on their Brownian motion.[4-6] The Ag bipyramids showed a bimodal distribution with modes at 60.191 and 116.44 nm. The Ag nanospheres small and large had modes at 98.78 and 139.55 nm, respectively. Size distributions are shown in Figure S1.

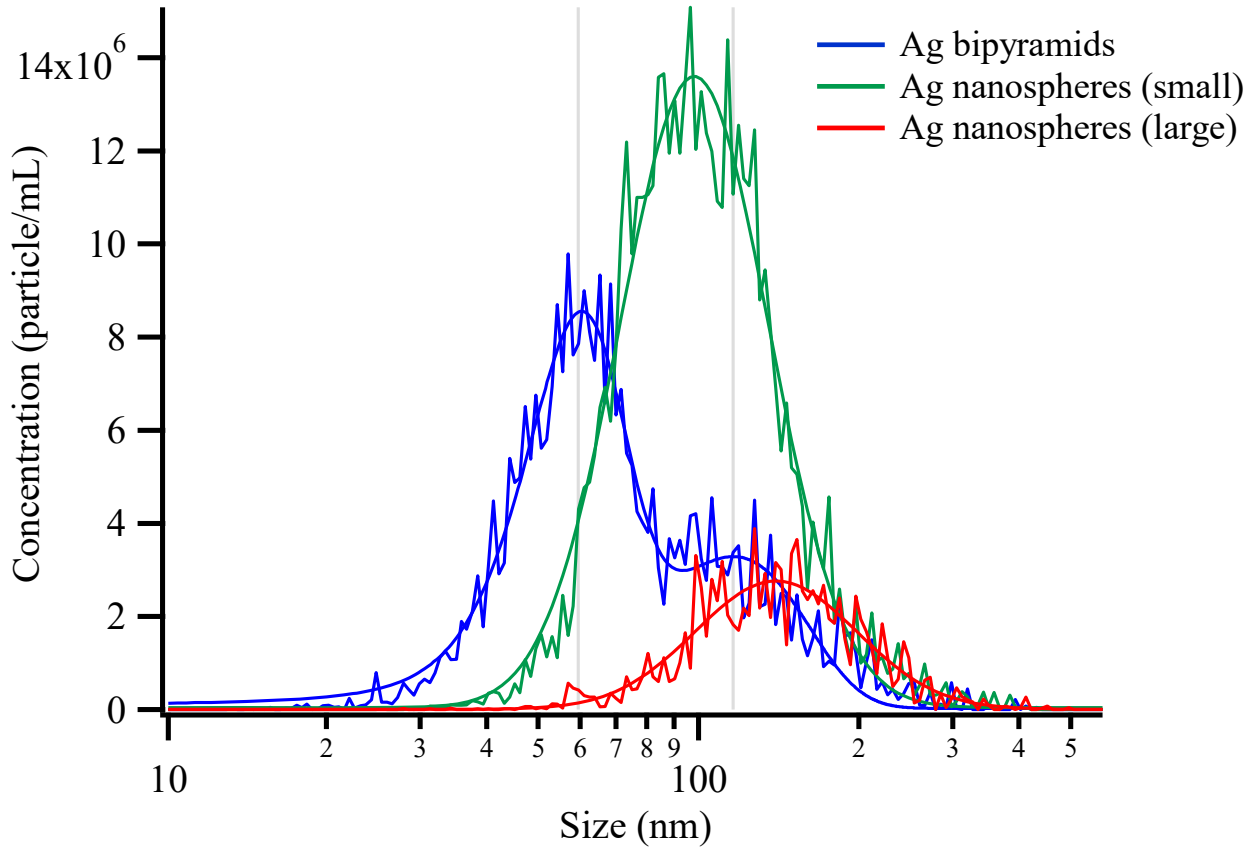

Figure S1. NTA size distributions (hydrodynamic diameter) of Ag nanoparticle colloidal solutions.

Laboratory-generated $(NH_4)_2SO_4$ particles were impacted onto the SERS substrates, as well as a plain quartz substrate and analyzed for SERS enhancement. Raman spectra were collected for 1 accumulation with 1 s acquisition time for the range of 200 – 1900 cm^{-1} and are shown in Figure S2. Similar to the substrate comparison discussed in the main text, the Ag foil SERS substrate yielded the best spectral enhancement. Enhancement factors for the $\nu(SO_4^{2-})$ mode were calculated to be 5.6, 3.1, 2.8, and 2.4 for the Ag foil, AgNPs (large), Ag bipyramids, and AgNPs (small), respectively.

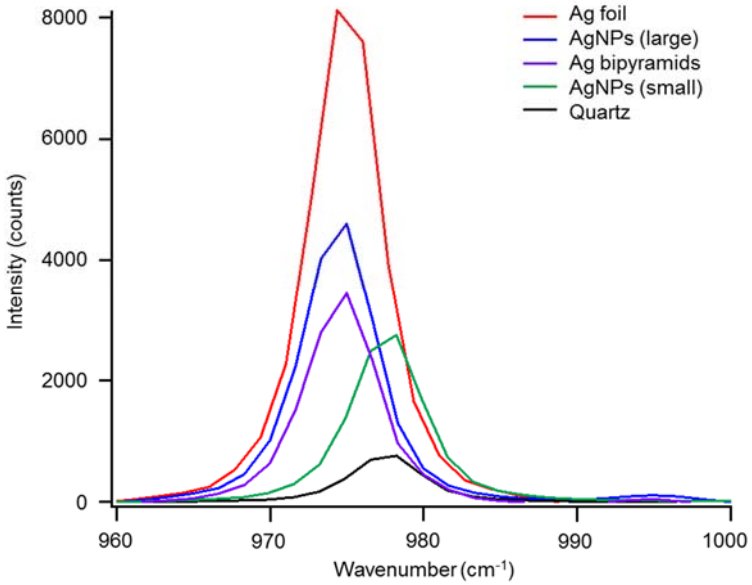

Figure S2. Comparison of Raman spectra of $(NH_4)_2SO_4$ particles for different types of Ag SERS substrates. Enhancement factors were calculated to be 5.6, 3.1, 2.8, and 2.4 for the Ag foil, AgNPs (large), Ag bipyramids, and AgNPs (small), respectively.

Ag Foil Characterization

For Ag foil substrates, small pieces were cut from a 2" x 7.50" x 0.002" Ag foil sheet. An optical, scanning electron microscopy (SEM) and atomic force microscopy (AFM) images (height and amplitude) of the Ag foil surface are shown in Figure S3. The roughness of the foil was ≤ 100 nm as seen from the heights in Figure S3c.

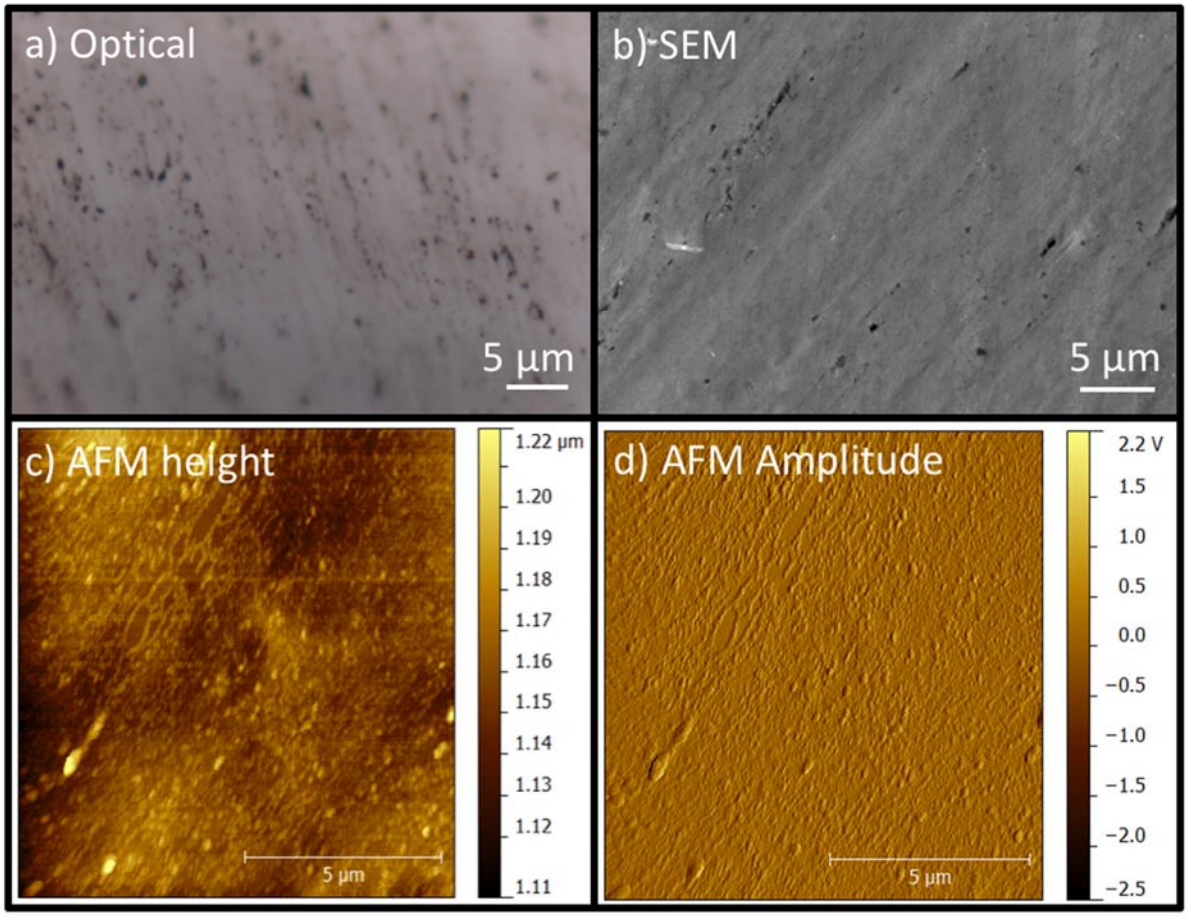

Figure S3. a) Optical, b) SEM, and c) AFM height, and d) AFM amplitude images of the Ag foil surface.

Raman Spectra

All Raman spectra and the average spectrum for 400 nm, 600 nm, and 800 nm PSL particles from both quartz and Ag foil substrates are shown in Figures S2-S4. All Raman spectra and the average spectrum for 400 nm, 600 nm, and 800 nm $(NH_4)_2SO_4$ particles from both quartz and Ag foil substrates are shown in Figures S5-S7. All Raman spectra and the average spectrum for 400 nm, 600 nm, and 800 nm $NaNO_3$ particles from both quartz and Ag foil substrates are shown in Figures S8-S10.

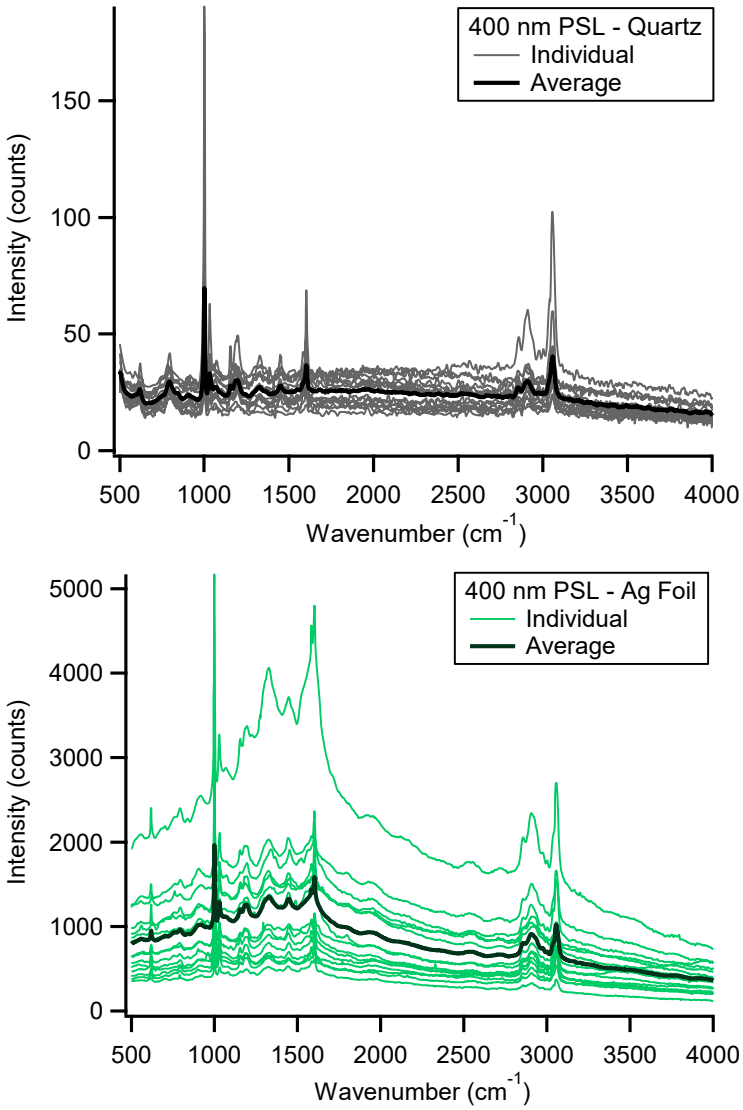

Figure S4. Raman spectra for 400 nm PSL particles on quartz (top) and Ag foil (bottom) substrates.

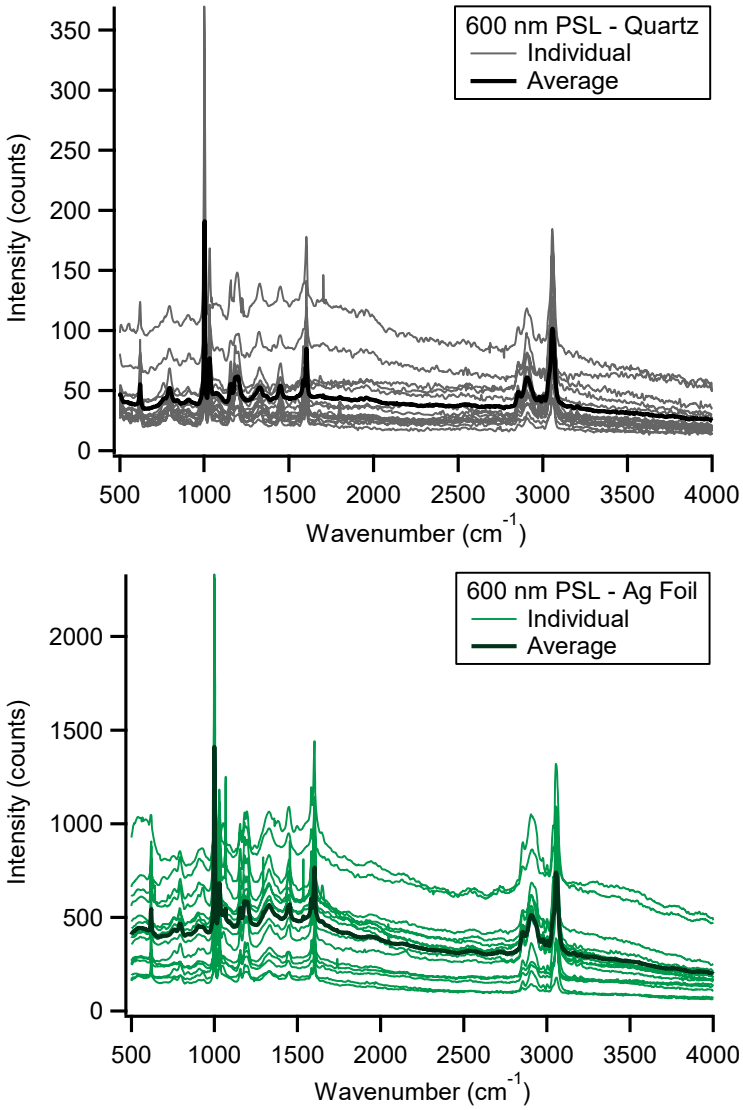

Figure S5. Raman spectra for 600 nm PSL particles on quartz (top) and Ag foil (bottom) substrates.

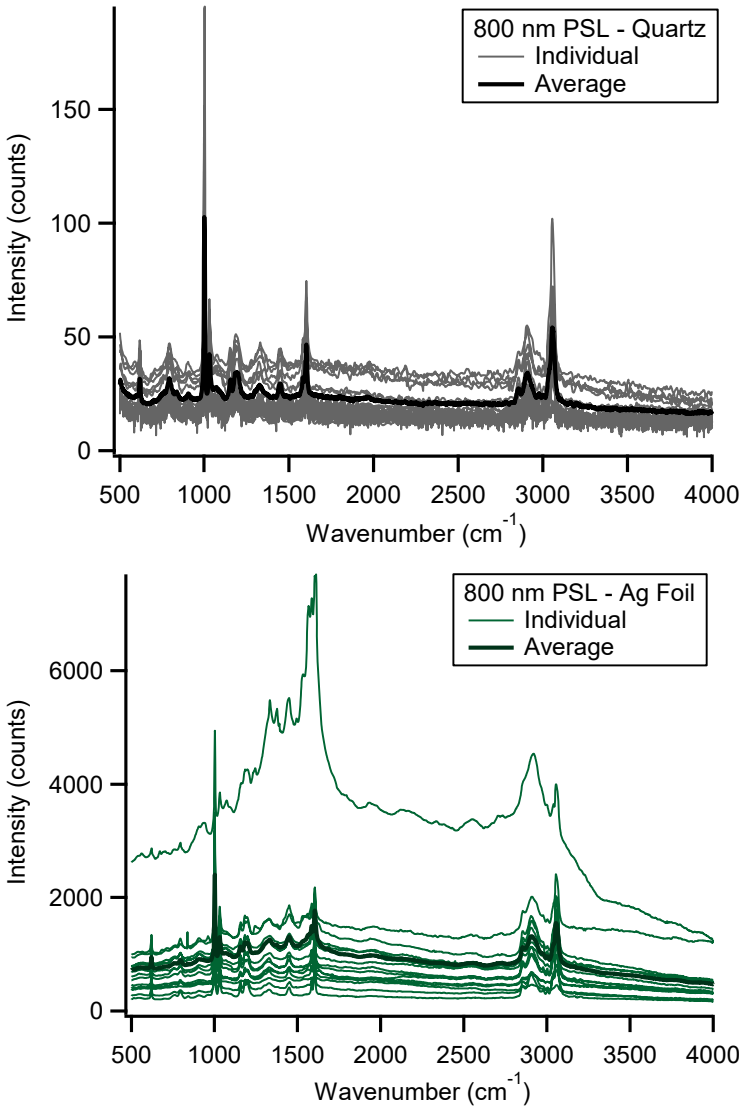

Figure S6. Raman spectra for 800 nm PSL particles on quartz (top) and Ag foil (bottom) substrates.

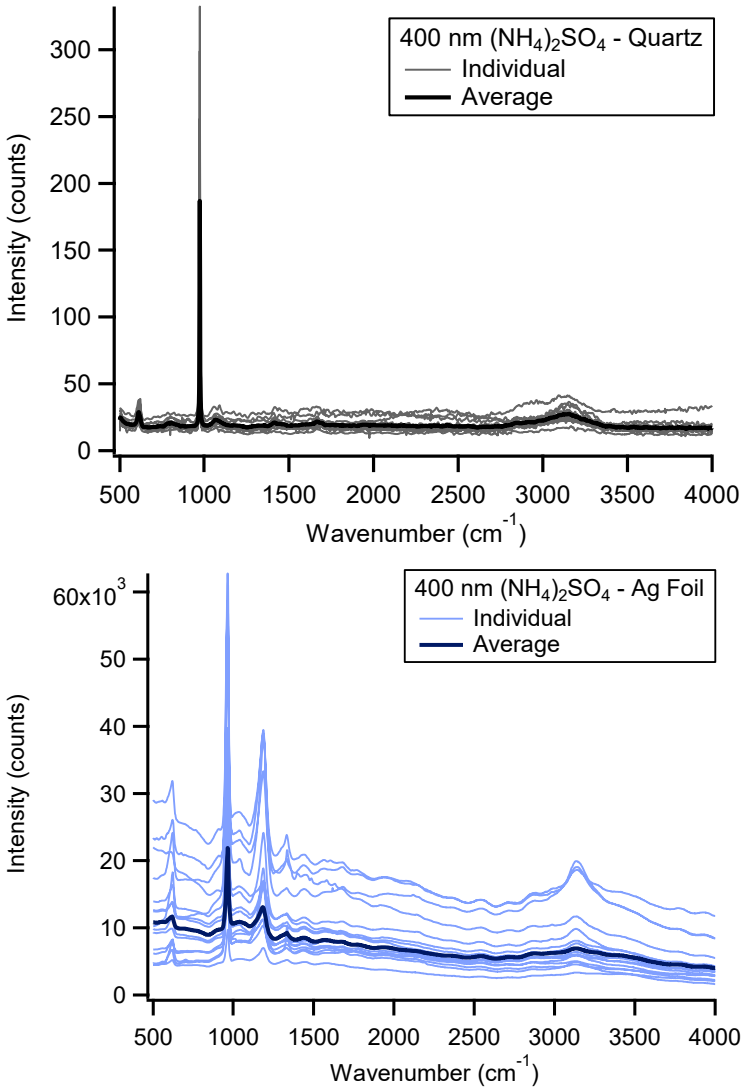

Figure S7. Raman spectra for 400 nm $(NH_4)_2SO_4$ particles on quartz (top) and Ag foil (bottom) substrates.

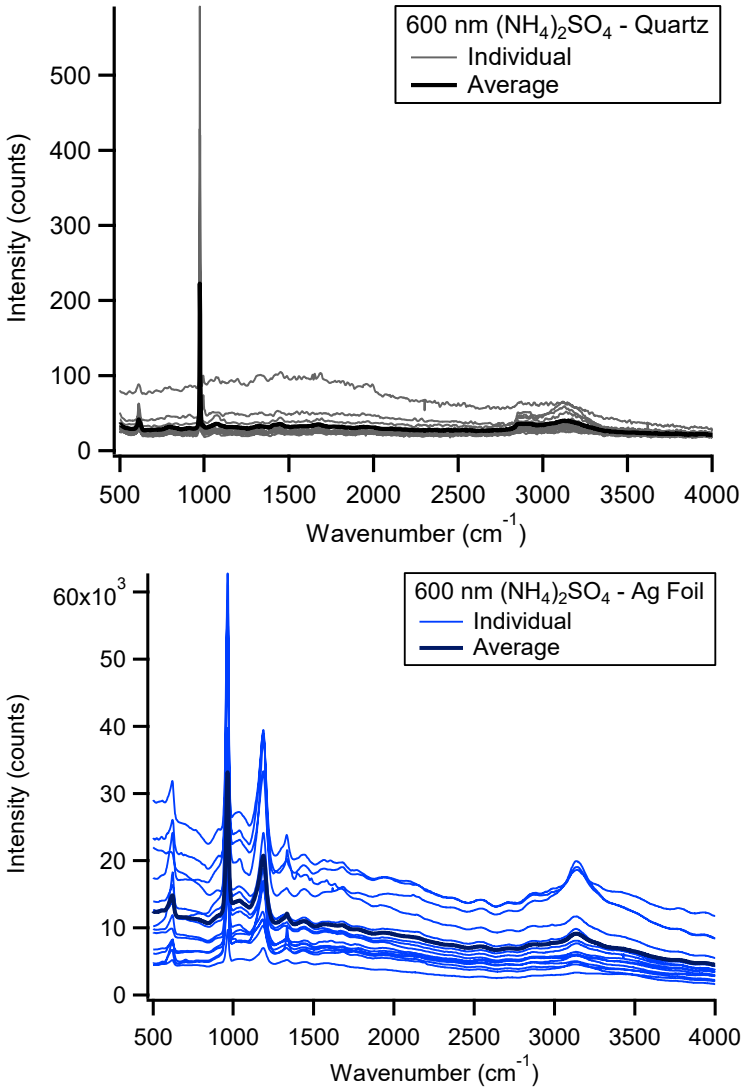

Figure S8. Raman spectra for 600 nm $(NH_4)_2SO_4$ particles on quartz (top) and Ag foil (bottom) substrates.

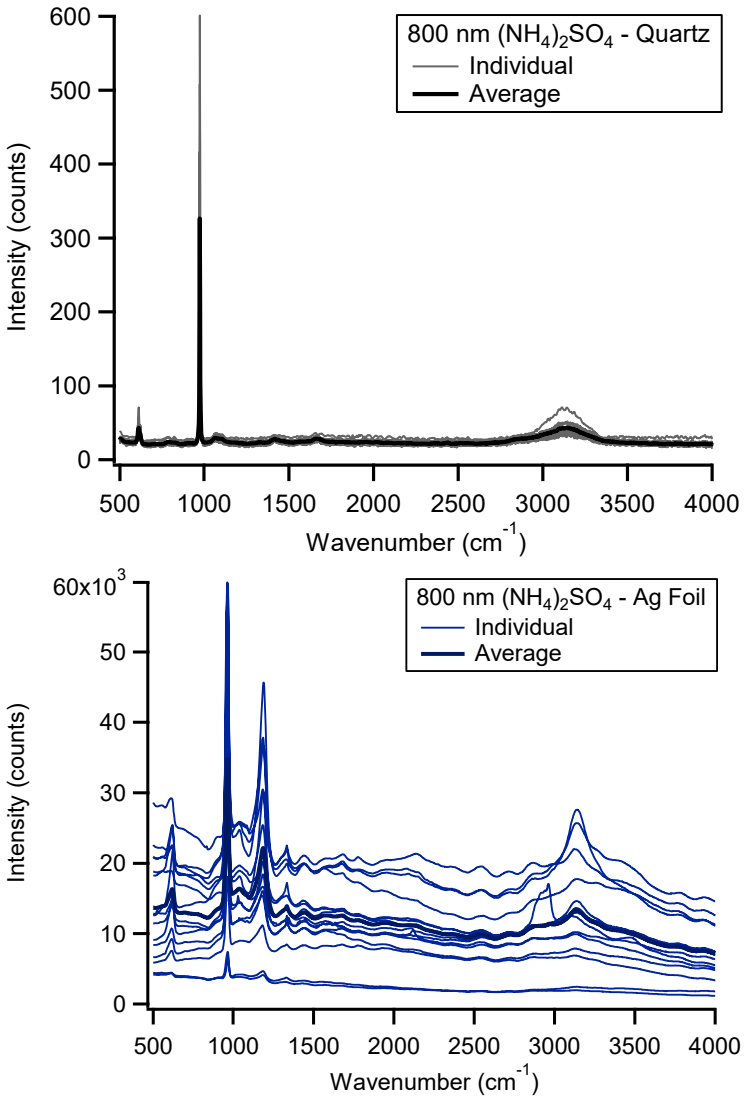

Figure S9. Raman spectra for 800 nm $(NH_4)_2SO_4$ particles on quartz (top) and Ag foil (bottom) substrates.

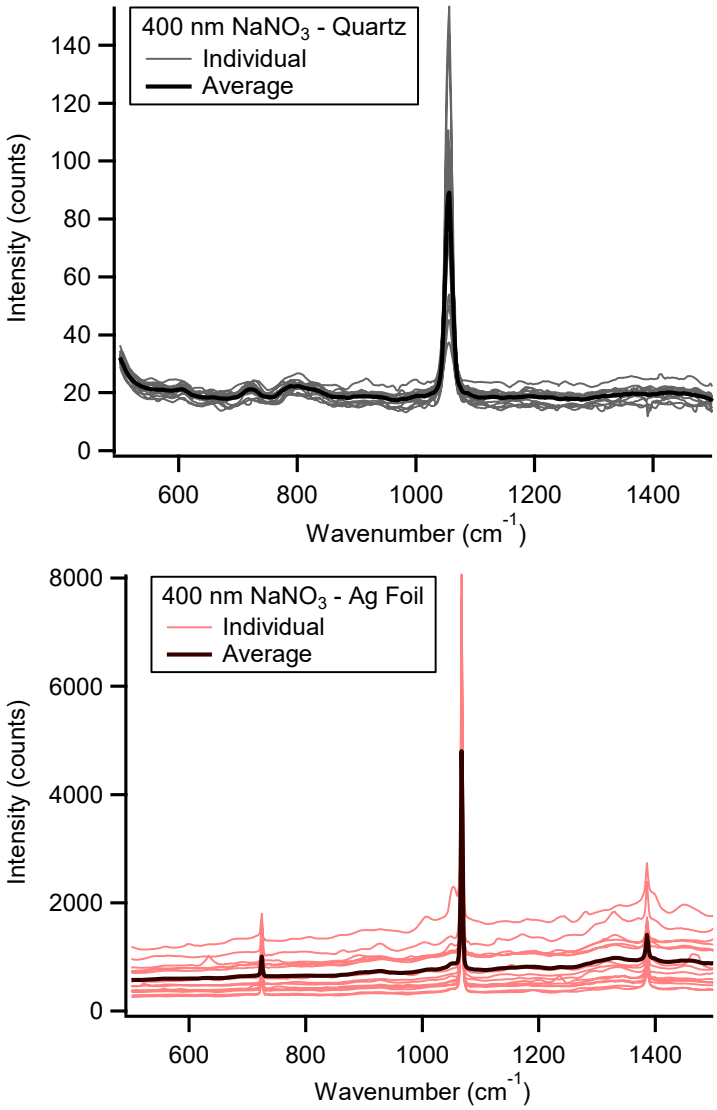

Figure S10. Raman spectra for 400 nm $NaNO_3$ particles on quartz (top) and Ag foil (bottom) substrates.

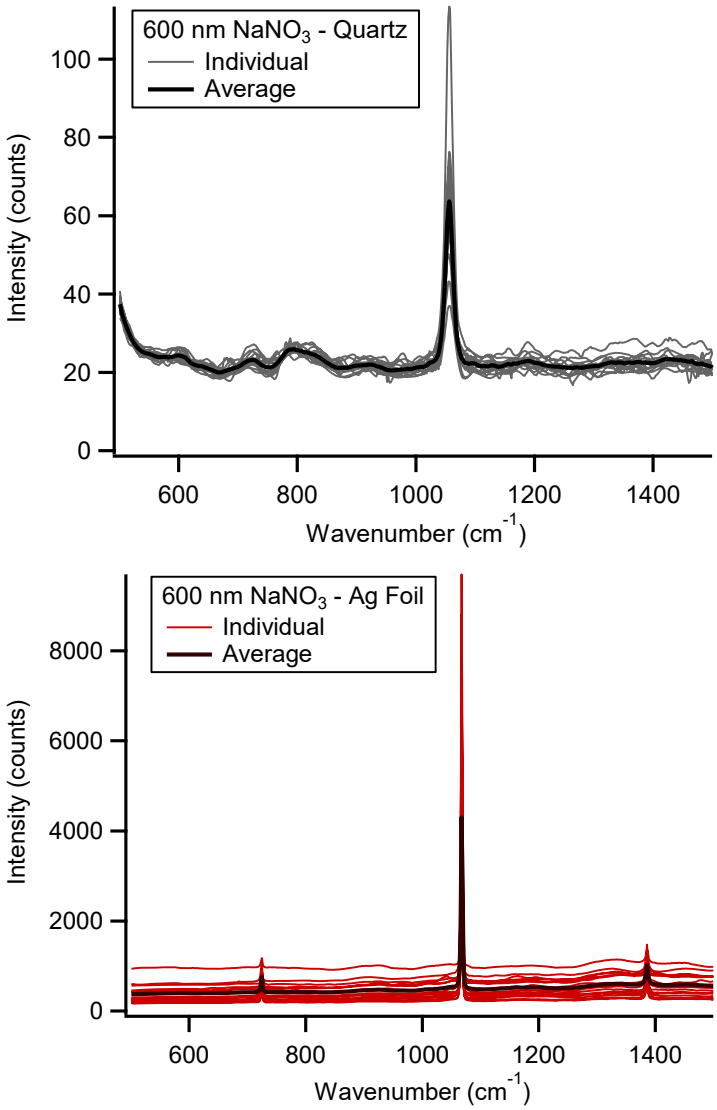

Figure S11. Raman spectra for 600 nm $NaNO_3$ particles on quartz (top) and Ag foil (bottom) substrates.

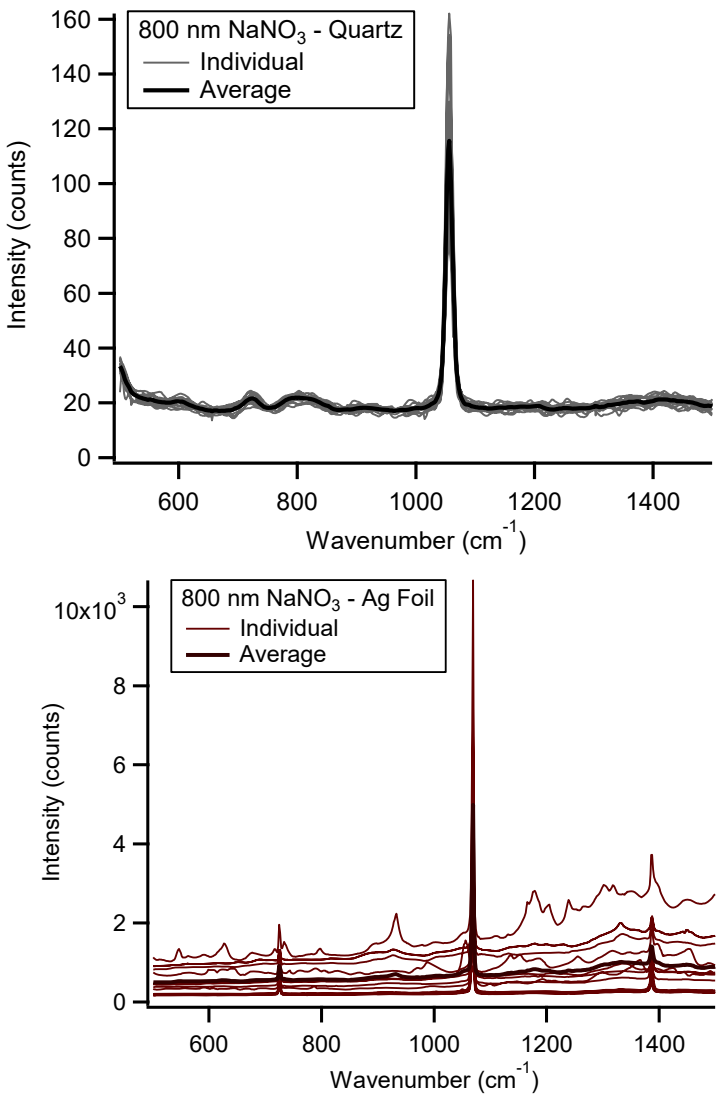

Figure S12. Raman spectra for 800 nm $NaNO_3$ particles on quartz (top) and Ag foil (bottom) substrates.

Ambient Aerosol Sample Optical Images

SERS spectra were collected for 150 nm size-selected ambient aerosol particles with point-by-point automated mapping with 0.25 μm step size. Figure S11 shows the Raman spectra and corresponding optical image for these sample with the mapped region and the location of the spectra highlighted. The ambient aerosol may appear larger in the optical image due to spreading upon impaction[7,8] or agglomeration, however, the large particles were avoided for this analysis.

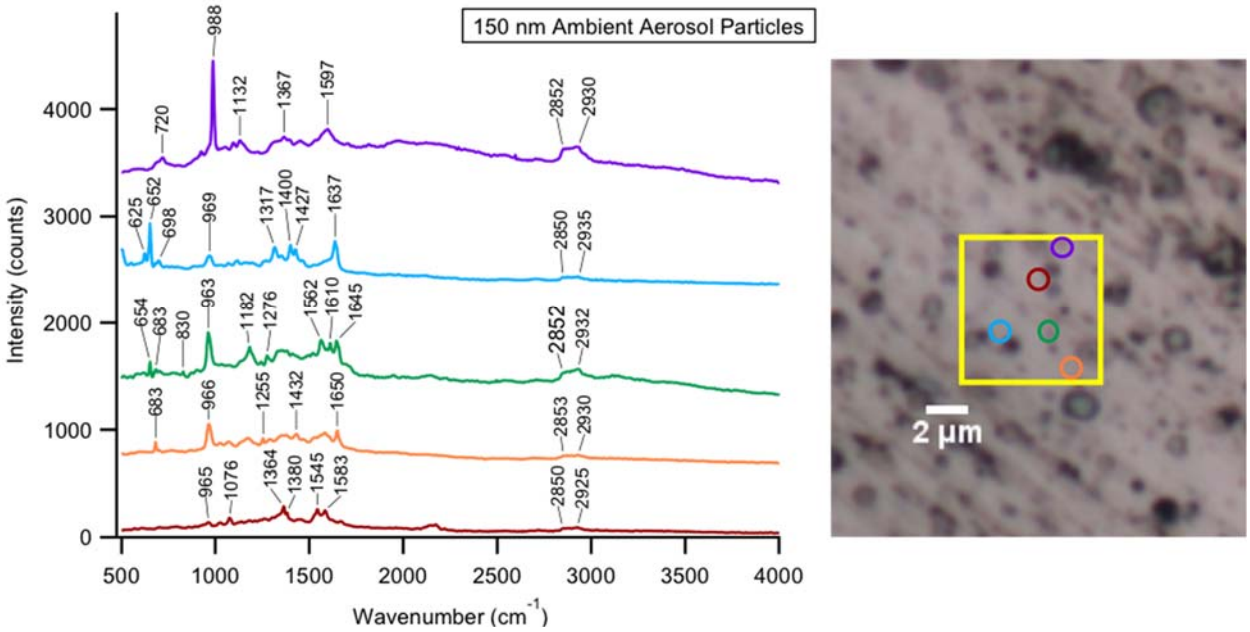

Figure S13. Raman spectra for 150 nm size-selected ambient aerosol particles with color coordinated highlights for their respective locations within the mapped region (indicated by the yellow square).

References

1. Leopold, N.; Lendl, B., A new method for fast preparation of highly surface-enhanced Raman scattering (SERS) active silver colloids at room temperature by reduction of silver nitrate with hydroxylamine hydrochloride. *Journal of Physical Chemistry B* **2003,** *107*, (24), 5723-5727.
2. Zhang, J.; Li, S.; Wu, J.; Schatz, G. C.; Mirkin, C. A., Plasmon-Mediated Synthesis of Silver Triangular Bipyramids. *Angewandte Chemie-International Edition* **2009,** *48*, (42), 7787-7791.
3. Craig, R. L.; Bondy, A. L.; Ault, A. P., Surface Enhanced Raman Spectroscopy Enables Observations of Previously Undetectable Secondary Organic Aerosol Components at the Individual Particle Level. *Analytical Chemistry* **2015,** *87*, (15), 7510-7514.
4. Bergin, I. L.; Wilding, L. A.; Morishita, M.; Walacavage, K.; Ault, A. P.; Axson, J. L.; Stark, D. I.; Hashway, S. A.; Capracotta, S. S.; Leroueil, P. R.; Maynard, A. D.; Philbert, M. A., Effects of particle size and coating on toxicologic parameters, fecal elimination kinetics and tissue distribution of acutely ingested silver nanoparticles in a mouse model. *Nanotoxicology* **2016,** *10*, (3), 352-360.
5. Ault, A. P.; Stark, D. I.; Axson, J. L.; Keeney, J. N.; Maynard, A. D.; Bergin, I. L.; Philbert, M. A., Protein corona-induced modification of silver nanoparticle aggregation in simulated gastric fluid. *Environmental Science: Nano* **2016,** *3*, (6), 1510-1520.
6. Axson, J. L.; Stark, D. I.; Bondy, A. L.; Capracotta, S. S.; Maynard, A. D.; Philbert, M. A.; Bergin, I. L.; Ault, A. P., Rapid Kinetics of Size and pH-Dependent Dissolution and Aggregation of Silver Nanoparticles in Simulated Gastric Fluid. *Journal of Physical Chemistry C* **2015,** *119*, (35), 20632-20641.

7. Bondy, A. L.; Kirpes, R. M.; Merzel, R. L.; Pratt, K. A.; Banaszak Holl, M. M.; Ault, A. P., Atomic Force Microscopy-Infrared Spectroscopy of Individual Atmospheric Aerosol Particles: Subdiffraction Limit Vibrational Spectroscopy and Morphological Analysis. *Analytical Chemistry* **2017,** *89*, (17), 8594-8598.
8. Sobanska, S.; Falgayrac, G.; Rimetz-Planchon, J.; Perdrix, E.; Bremard, C.; Barbillat, J., Resolving the internal structure of individual atmospheric aerosol particle by the combination of Atomic Force Microscopy, ESEM-EDX, Raman and ToF-SIMS imaging. *Microchemical Journal* **2014,** *114*, 89-98.